CHAPTER 8

Formation and Growth of Bulk Phases

8.1 INTRODUCTION

If monolayer formation processes deal with the most intricate fundamental problems in electrochemical surface science, formation of bulk phases on the electrode surfaces is probably the most important process from technology point of view. Electrometallurgy, electroplating and metal finishing, anodizing, corrosion and corrosion protection, battery and fuel cell electrodes are only some examples of the conventional areas in electrochemistry where bulk phase formation is involved. Conducting and nonconducting polymer film formation on metal and metal oxide electrodes and the formation of photoactive semiconductors are some new areas of research in these lines.

In such a multidisciplinary area of research, people with very different research interests try to obtain bulk phases with widely differing physicochemical properties. Metallurgists, for example, are interested in producing thick metal deposits at minimum energy costs. Metal platers, on the other hand, are interested in obtaining a uniform bright and fairly thin metal deposit. Corrrosion scientists are interested in obtaining a protective insulating phase whereas battery scientists are interested in a conducting and reactive phase formation. A semiconducting material is of interest to photoelectrochemist. In the formation of polymer film, a similar variation in research interests may be noticed. Because of such varied interests and requirements, electrochemical formation of cathodic and anodic deposits of a wide variety of metals, metal oxides, sulphide, metallic salts, non-metallic materials and polymers are being investigated today. One would not expect that all these bulk phase formation processes would follow a single model. Among the types of electrochemical processes considered in this monograph, formation of bulk phases, in fact, requires maximum number of model components to describe the behaviour of different materials under different experimental conditions. Although each model has been extensively developed by different groups of specialists, the authors are not aware of any work that has even attempted to categorize the bulk phase formation processes in a balanced and objective fashion. Hence, an attempt has been made to introduce the models involved in the bulk phase formation in a general fashion (Section

8.2.1) and then to discuss the individual models in some detail (Rest of Section 8.2).

Since this is the state of affairs in the modelling level itself, it is hardly surprising that the voltammetric methods for distinguishing between these models have not developed substantially. By evaluating the available literature and using the methods discussed so far for other types of processes, an approach for distinguishing these models by LSV and CV techniques are then presented in Section 8 3. The experimental results are analyzed at present with a lot of subjectivity (Section 8.4). The widest scope for developing LSV and CV techniques and for that matter any other technique, such as impedance for the study of the different bulk phase formation models are made apparent throughout this discussion. It is hoped that such a discussion would induce further works in this fascinating, technologically important and indeed very challenging area of research.

8.2 THE MODEL

Bulk phases may be formed on electrode surfaces by a number of seemingly unconnected reaction mechanisms. Perhaps for this reason, no comprehensive discussion or even a systematic classification of the types of processes involved are found in the literature. Broadly, bulk phase formation processes may be classified into four major groups: (a) formation and growth without any chemical changes of the electrode substrate; (b) Formation of phases involving chemical changes of the electrode surface; (c)growth of phases involving chemical changes of the electrode surface; and (d) formation and growth of phases with other parallel chemical reactions.

Even before discussing the model parameters and relevant basic equations (as in the second section of each chapter) it is felt desirable here to present a brief and unified account of all these models and the model components involved in each model. In such a discussion, one can fortunately notice that many of the so-called 'different models', after all, are composed of much smaller number of model components, many of which are already introduced in earlier chapters. All the models and the model components of bulk phase formation and growth processes are also consolidated in Table 8.1

Table 8.1

Models of electrochemical phase formation and growth

No	Model	Model components
1	Electrodeposition of metal on liquid surface	Charge transfer, dlffusion in bulk phases (Chapter 6)
2	Layer by layer growth of conducting films	Charge transfer, monolayer surface coverages (Chapter 7)
3	Deposition on non-uniform solid substrate	Charge transfer, surface diffusion (Ref 1—6)
4	Deposition on uniform surfaces	Charge transfer, Nucleation, growth, diffusion
5	Deposition of conducting non-metallic films	Charge transfer, chemical reaction (polymerization)
6	Deposition of insulating films	Charge transfer, chemical reaction, film resistivity
7	Anodic film formation-direct deposition	Charge transfer, chemical reaction
8	Anodic film formation-dissolution preciptiation	Charge transfer, chemical reaction (precipitation), film resistivity, diffusion
9	Film growth-pore diffusion	Charge transfer, chemical reaction (precipitation), pore diffusion
10	Film growth-solid state diffusion	Charge transfer, chemical reaction, solid state diffusion
11	Film growth-place exchange	Charge transfer, place exchange
12	Film growth-surface roughening	Charge transfer, irreversible place exchange
13	Film growth-ionic migration	High field growth

8.2.1 THE HIERARCHY OF MODELS

Consider the simplest electrochemical phase formation process namely, the electrodeposition of metal on an inert substrate.

$$M^{n+} + ne \rightleftharpoons M \qquad 8.1$$

Even this process may take place by different routes depending on the nature of the solid substrate. Even a macroscopically smooth single crystal electrode surface contains a number of surface defects such as pits, ledges and kink sites as depicted in Fig. 8.1. If the metal adatom M formed by reaction 8.1 reaches a kink site, for

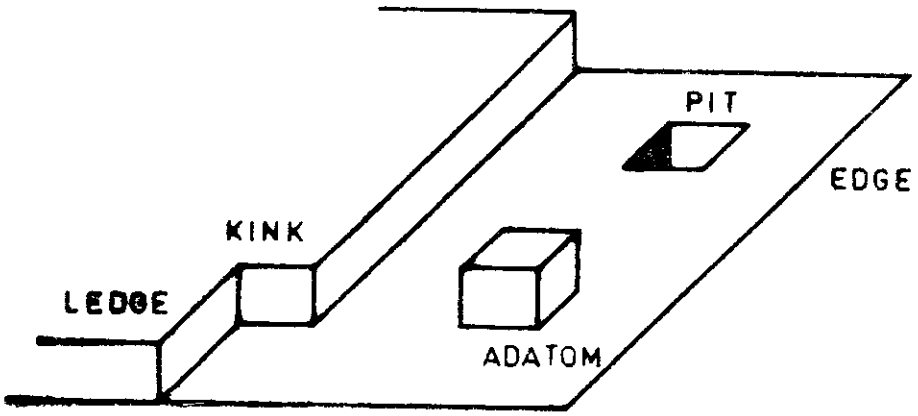

Fig. 8.1 Surface defects and surface sites on a well defined single crystal electrode surface Other defects such as dislocation are not indicated.

example. it is more likely to stay there rather than dissolve back because it is held by more number of nearest neighbours. Comparatively, the adatom deposited on the plane would be less stable. If the substrate electrode contains relatively large number of active centres such as kink sites, all the electroreduced metal adatoms would be incorporated into the substrate lattice. No specific overvoltage is then required for such phase formation. Such metal deposition and dissolution models on uniformly active solid or liquid electrodes were considered in Chapter 6 and hence do not receive any further consideration here.

When sufficient number of such active centres are not available on the electrode surface, the adatoms are likely to encounter a plane electrode surface, and they would have to diffuse through

considerable distance on the surface of the substrate to reach a ledge or a kink site. This phenomenon of surface diffusion of adatoms have received considerable attention in the past [1–6]. This model also has substantial experimental support since a number of deposits are observed as platelets and spiral growth patterns which can only be explained by this model [1–6]. However, the 'surface diffusion' phenomena cannot be easily distinguished from the bulk diffusion of metal ions unless the diffusion coefficients are very different [7]. Authentic surface diffusion coefficients in electrodeposition conditions are not available at present to verify this fact. In this context, the voltammetric technique like any other electroanalytical technique cannot distinguish surface diffusion controlled processes from bulk diffusion controlled processes discussed above. Hence this model is not considered in any detail further.

If the electrode surface is extremely smooth, the adatoms formed must join together to form discrete nuclei (Section 8.2.3) which can grow further (Section 8.2.4). This type of model is fairly well understood and voltammetric methods have also been developed well (Section 8.3.1).

Apart from metals, organic and inorganic molecular species may also polymerize on an inert electrode surface. If the polymer formed is conducting, then the voltammetric responses would be very similar to the nucleation growth processes discussed above. However, as is discussed later (Section 8.2.4), the phase growth is now due to a subsequent potential-independent chemical reaction (Section 8.2.5). If the polymer film is insulating in character, the voltammetric response would be very similar to monolayer formation processes discussed in Chapter 7 but the model parameters would now have a different meaning (Section 8.3.2).

A number of metal electrodes are reactive and form oxide, sulphide or halide phases during anodic polarization. The initial stages of these phase formations may be interpreted in three models: the nucleation growth (Section 8.3.1) of the reactive phase; direct deposition of the anionic species (Section 8.3.2); and, the formation of a new insoluble chemical phase after dissolution of the metal (Section 8.3.3). The latter model is generally known as dissolution-precipitation model.

Once such a non-metallic phase is formed on an electrode surface, further charge transfer occurs through this phase. The phase growth

under these conditions can occur at least by five mechanisms. The metal cations may diffuse from the metallic side to the electrolyte side of the interface or the counter-ions might move in the opposite direction. If the non-metallic phase is porous, this diffusion might be through the pores. If the non-metallic phase is compact, solid state diffusion may take place (Section 8.2.6). The solid state phase exchange may also account for the growth of a new phase (Section 8.2.7). By repeated formation of such a place exchanged oxide and its reduction at very fast rates, one can roughen the electrode surface and by this means one may, in fact, be able to grow very thick oxide phases (Section 8.2.8). Finally, if the film is a compact dielectric material, the oxide may grow by a field-dependent migration process alone (Section 8.2.9).

So far in this discussion, it has been assumed that bulk phases are formed by a single electrochemical process. More often, however, one encounters parallel electrochemical processes. For example, along with formation of Fe $(OH)_2$ phase on iron one may notice parallel oxidation of Fe $(OH)_2$ to FeOOH. Another possibility is the simultaneous formation of a new phase along with its own dissolution. Many active metal dissolution processes may follow this route. Phase growth also may be accompanied by other parallel electrochemical reactions such as oxygen evolution or oxidation of other organic compounds. Distinct voltammetric methods may not be developed for such parallel processes in the near future. The overall response would be the combination of the individual processes. In practice some subtle approaches may be adopted to decouple phase growth processes from the overall response.

8.2.2 CHARGE TRANSFER

In the bulk phase formation processes, three types of charge transfer reactions are generally encountered. Deposition of metal M on the subtrate of the same or different electrode (S) is the common process in metallurgical and metal plating industry.

$$S + M^{n+} + ne \rightleftharpoons S - M \qquad 8.2$$

Anodic phase growth involves the direct deposition of an anionic species with simultaneous oxidation of metal M to form an ionic or covalent species MX.

$$M + X^{n-} \rightleftharpoons M - X + ne \qquad 8.3$$

In electropolymerization processes, both the oxidized and reduced monomeric species are solution-soluble (8.4). The phase growth in such cases occurs through a chemical polymerization reaction step (Section 8.2.5)

$$A + ne \rightleftharpoons A^{n-} \qquad 8.4$$

The charge transfer kinetics for all these cases is described again by Butler-Volmer relation (Section 4.2).

$$\frac{i}{nFA} = k_h^o [C_{Ox} \exp\{-\alpha n_a f(E - E^f)\} - C_R \exp\{(1-\alpha) n_a f(E - E^f)\}] \qquad 8.5$$

and the charge transfer equilibrium is described by Nernst relation (Section 3.2)

$$E_{eq} = E^f + \frac{\mathbf{R}T}{nF} \ln \frac{C_{Ox}}{C_R} \qquad 8.6$$

The oxidized and reduced species in equations 8.2 to 8.4, of course, are quite obvious. In metal deposition processes on its own substrate metal, the concentration of reduced metal is generally taken as unity. Similarly in reaction 8.3, the C_{ox} (that is the concentration of $M-X$) is taken as unity. This is because these surface concentrations do not change with time. This assumption can be easily introduced in equations 8.5 and 8.6 for the corresponding processes.

8.2.3 NUCLEATION

As mentioned earlier (Section 8.2.1) if the deposition is to take place on a defect-free surface, individual adatoms or even very small adatom clusters would dissolve back because the new phase would not be stable. A critical nucleus containing at least N_c number of adatoms must be formed first to remain as a stable phase. If one assumes that the critical nucleus is spherical in shape and the charge transfer involved in critical nuclei formation (equation 8.7) is reversible, N_c, the number of adatoms in the critical nuclei and ΔG_c, the free energy of nuclei formation are given by equations 8.8 and 8.9 respectively [8–10].

$$N_c . M^{n+} + N_c\, ne \rightleftharpoons M_{N_c \text{ cryst}} \tag{8.7}$$

$$N_c = \frac{288\ \pi\ v_m^2 . \sigma^3}{27\ (ne_o\eta)^3} \tag{8.8}$$

$$\Delta G_c = \frac{144\ \pi\ v_m^2 . \sigma^3}{27\ (ne_o\eta)^2} \tag{8.9}$$

In these expressions, v_m is the volume occupied by one atom in the crystal and σ is the effective surface free energy of the nuclei.

The effective rate of three dimensional nuclei formation ($k_{n,3}$) at any given overvoltage is given by

$$k_{n,3} = k^o_{n,3} \exp\left(\frac{-\Delta G_c}{kT}\right)$$

$$= k^o_{n,3} \exp\left(\frac{-b}{n^2\eta_c{}^2}\right) \tag{8.10}$$

where $b = 144\ \pi \cdot v_m^2 \cdot \sigma^2/27\ e_o^2 \cdot kT$ is a constant value at any temperature. The nucleation rate versus $1/\eta_c^2$ ralation has been verified for a few nucleation processes and a brief review is also available [10].

In a heterogeneous electrode surface, the nuclei can be formed only on certain critical sites, N_o. The number of nuclei at any point of time $N(t)$ is given by

$$N(t) = N_o \cdot \exp(-k_{n,3} \cdot t) \tag{8.11}$$

This expression again has two limiting conditions. When $k_{n,3}$ is very large, all the nuclei are formed instantaneously.

$$N(t) = N_o \text{ (Instantaneous nucleation)} \tag{8.12}$$

If $k_{n,3}$ is very small, $N(t)$ increases with time depending on the value of $k_{n,3}$. By linearizing (equation 8.12) one abtains the expression for $N(t)$ under the progressive nucleation conditions.

$$N(t) = N_o\ k_{n,3} \cdot t \text{ (progressive nucleation)} \tag{1.13}$$

One may note that the three-dimensional nucleation model introduced in this section is very similar to the two-dimensional nucleation model introduced in the last chapter (Section 7.2). In fact the concept of two dimensional nucleation was developed from the conceptual framework of three dimensional nucleation.

Although the nucleation model was introduced using metal deposition process, the model as such is a general one and is applicable for anodic phase formation processes [11] as well.

8.2.4 GROWTH

Another important aspect in solid state phase growth is the fact that the area of the growth process itself changes with time. When the three-dimensional metallic nuclei are formed on an electrode substrate, for example, the effective surface area keeps on increasing with the increase in the number of nuclei formed as well as their area increase.

The growth process can be modelled by considering the behaviour of each individual growth sites. The growth site can have various geometries and time-dependent growth expression for a number of growth geometries such as hemispherical, conical and cylindrical ones which have been considered in the metal deposition context itself [12, 13]. Consider the hemispherical geometry alone here.

The radical growth expression for an electron-transfer process (equation 8.14) can be written as equation 8.15 which again is similar to the two-dimensional growth law expressed earlier (Section 7.2.)

$$(M)_{\text{cryst}} + M^{n+} + ne \rightleftharpoons (M)_{\text{cryst}} - M \qquad 8.14$$

$$\frac{dR}{dt} = \rho_v^{1/3} k_g^o [\exp\{-\alpha n_a f(E - E^f)\} - \exp\{1 - \alpha) n_a f(E - E^f)\}] \qquad 8.15$$

In this expression ρ_v is the volume occupied by each individual metallic species and all other symbols have their usual meaning.

Now the volume of the crystal at any time $V(t)$ may be written using equation 8.15

$$V(t) = \frac{2\pi}{3} \int_r^t \left(\frac{dR}{dt}\right)^3 dt. \qquad 8.16$$

The current due to the growth process at any point of time t is related to the rate of change of $V(t)$ with respect to time by the following expression

$$i = \frac{nF}{V_m} \cdot \frac{dV}{dt} \qquad 8.17$$

where V_m is the molar volume of the crystalline deposit formed.

Again, the above model for the growth process involving increase in surface area can be directly used for anodic dissolution processes as well. In deposition processes, the size of the deposit grows with time whereas in the dissolution process the size of the pit increases with time (Fig. 8.2). In the model level, both these processes,

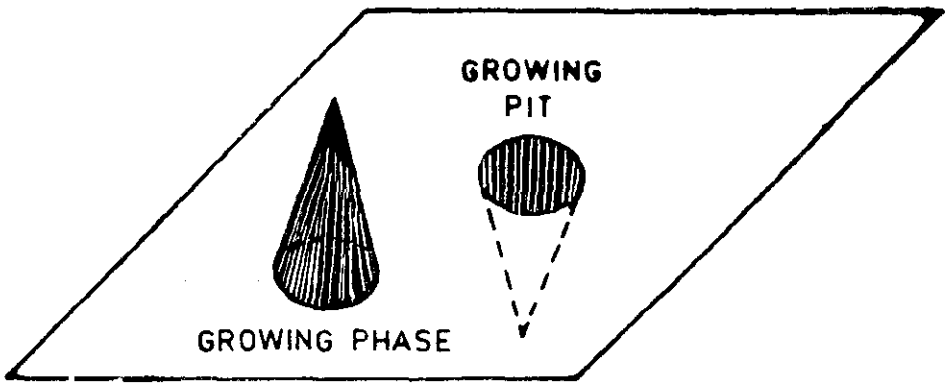

Fig. 8.2 Growth of a conical phase and pit.

however, are identical. Growth expressions of the type suggested above have also been used frequently for conducting polymer formation. However, the polymerization reaction should rather be thought of as a chemical reaction (Section 8.2.5) followed by charge transfer. No serious efforts to develop growth expressions for such potential-independent steps are noticed in literature.

8.2.5 CHEMICAL REACTION

Consider dissolution of metal M as M^{n+} in an anodic process (reaction 8.2). The dissolved metal ion can now react with an anionic species X^{n-} in solution to form MX

$$M^{n+} + X^{n-} \underset{k_b}{\overset{k_f}{\rightleftharpoons}} MX. \qquad 8.18$$

The overall effect of these two steps is a film formation process. Now the precipitation reaction (equation 8.18) may simply be considered as a chemical reaction

$$v = k_f . C_{Mn+} . C_{Xn-} - k_b . C_{MX} \qquad 8.19$$

The chemical reaction rate constants, of course, are potential-independent.

The polymerization following the charge transfer step (equation 8.4) is also a chemical step.

$$aA^{n-} \rightleftharpoons (A)_a^{an-} \qquad 8.20$$

However, the polymerization is usually accompanied by other chemical steps such as protonation (8.21), deprotonation, hydroxylation etc.

$$(A)_a^{an-} + anH^+ \rightleftharpoons (AH_n)_a \qquad 8.21$$

Hence the overall polymerization processes are generally irreversible chemical steps. On the other hand, the precipitation reactions are reversible in character.

Dissolution-precipitation reactions and electropolymerization reactions can be treated using the methods discussed for the study of EC_r and EC_{irr} reactions in Chapter 5. However, the treatments presented there do not involve change in electrode area with time. The dissolution-precipitation and conductive polymer formation processes involve increasing electrode surface area with time. The insulating polymer formation involves decreasing electrode area with time. This important difference can affect the voltammetric behaviour to a very great extent. This aspect requires some detailed consideration.

8.2.6 DIFFUSION

Although one encounters diffusion in the liquid phase, diffusion over the surface, diffusion on compact solid phase and diffusion through pores in bulk formation processes, the basic equations used to describe them are the well-known Fick's first and second laws only.

$$v = -D \cdot \frac{\partial C}{\partial x} \qquad 8.22$$

$$\frac{\partial C}{\partial t} = D \frac{\partial^2 C}{\partial x^2} \qquad 8.23$$

This is because the basic driving force in all these cases are only concentration gradients. Depending on the type of medium, the range of values for diffusion coefficients may vary. The solution phase diffusion coefficients are around 10^{-5} cm^2/sec. The D values through pores and surface diffusion coefficients also probably fall

in this range of values. The solid state D values can reach as low as 10^{-10} cm^2/sec or even lower.

8.2.7 PLACE EXCHANGE

If the metal atoms do not dissolve, and re-precipitate, an oxide layer to the maximum extent of one monolayer thickness can grow by direct deposition mechanism. For the oxide growth, a further mechanism is required. An oxide can grow at least by three means. One is the solid state diffusion of cations and anions discussed above (Section 8.2.6). In this and the next section, the oxide growth by place exchange are considered.

The mechanism of place exchange is illustrated in Fig. 1.13. The metal cation and oxide anions exchange their places simultaneously. Consider that for the exchange of a pair of metal ions and oxide ions, an activation energy $\Delta G_{ex}^{\neq}$ is required. At any point of time, if there are x layers, the rate of growth of thickness $L(t)$ is given by

$$\frac{dL(t)}{dt} = k_{ex,L} = k_{ex,O} \cdot \exp\left(-\frac{x\Delta G^{\neq}}{2\mathbf{R}T}\right) \qquad 8.24$$

In this equation, $k_{ex,L}$ is the rate constant at any length L of oxide layer thickness and $k_{ex,O}$ is the rate at $L = 0$. The factor 1/2 appears in the exponent because of the simultaneous movement of cations and anions [12]. In this equation, the number of layers x is related to the thickness of the layer L and width of each metal oxide layer w by the following equation.

$$x = \frac{L}{w} \qquad 8.25$$

Hence the oxide growth rate decreases as L or x increases.

The growth rate is related to the current by the following expression

$$i = q_m \cdot \frac{dL}{dt} \qquad 8.26$$

where q_m is the charge required for the formation of oxide layer of unit thickness.

One must note that the oxide growth rate when $L = 0$ is still a function of potential at the electrode-electrolyte interface. One can write a Butler-Volmer relation for $k_{ex,o}$

$$k_{ex,o} = k^{o}_{ex,o}\ [\exp\{\beta nf(E-E^{f})\} - \exp\{-(1-\beta)nf(E-E^{f})\}] \qquad 8.27$$

However, under constant potential conditions, $k_{ex,o}$ is independent of potential and equation 8.24 can be directly integrated using equation 8.25 and the condition that at $t = 0$, $L = 0$. One can get a linear relation between L and $\log t$.

$$L = A + B \log t \qquad 8.28$$

Hence this oxide growth law is termed as the direct oxide growth law.

The type of growth processes is noticed when the oxides formed possess some ionic character. This law was firmly established using oxide growth on iron in the passive region [12]. A number of other oxides also show this type of behaviour. However, there is still a lot of controversy on whether these systems follow place exchange mechanism mentioned here or ion-migration mechanism (Section 8.2.9).

8.2.8 SURFACE ROUGHENING

What would happen when an oxide formed by place exchange process is again reduced? The events that take place at different time

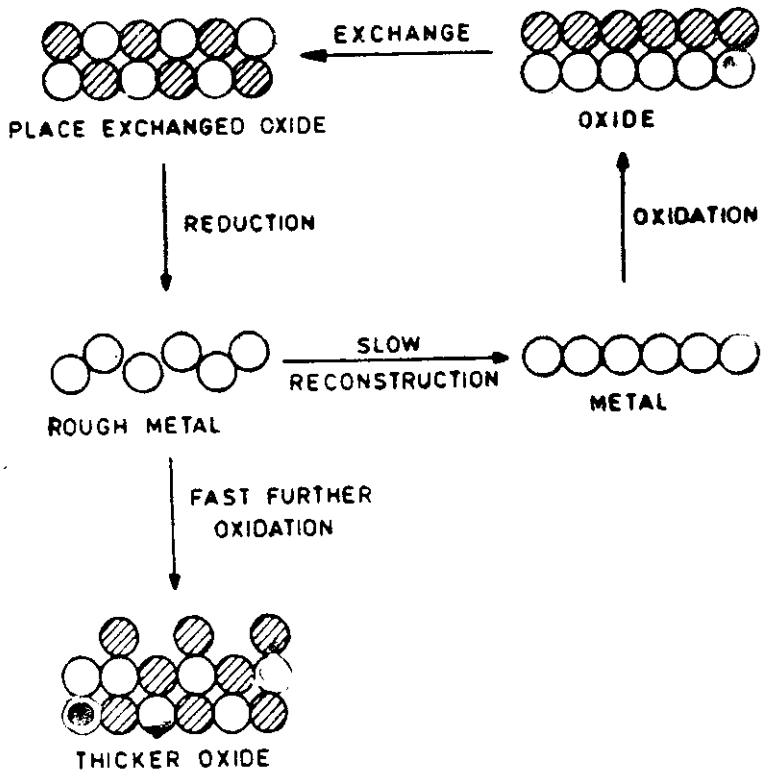

Fig. 8.3 Mechanism of oxide growth by surface roughening.

scales are presented in Fig. 8.3. When the complete monolayer of oxide is formed (Fig. 8.3a), a small fraction undergoes place exchange and a few metal atoms come out to the surface (Fig. 8.3b). Now, if the oxide is suddenly reduced, one notices a reconstructed rough metal surface (Fig 8.3c). If sufficient time is allowed, this roughness may be removed as the metal atoms revert back to their original places (Fig. 8.3d).

However, if the metal in the rough reconstructed state (Fig. 8.3c) is again reoxidized quickly, more oxide may be formed without place exchange itself (Fig. 8.3e). Hence by a continuous fast oxidation and reduction of oxide layers under place exchange conditions, one can produce a very thick oxide layer.

This type of oxide growth by a fast potential sweep has been attempted on a number of noble metal oxides (Section 8.4.4). However, the process has not been mathematically described yet. This is essentially a place exchange process, where the electrode area also is a function of time.

8.2.9 SOLID STATE IONIC MIGRATION

One should always be aware of the field strength that exists at electrochemical interfaces. Even if a potential of 0.1 V is applied across an interface, in the space between one metal atom layer and an oxygen atom layer which is in the order of 10^{-8} cm, the field strength is 10^7 V cm^{-1}. Such a high field can essentially induce ionic migration. This field can move metal cations away from the metal lattice and oxide anions towards the metal lattice.

The model for the growth of an oxide film in presence of a field gradient is presented in Fig. 1.16. The rate expression may again be written as

$$\frac{dL}{dt} = k_{fg} = k^{o}_{fg}\left[\exp\left(\frac{n\,l\,f\,E}{L}\right) - \exp\left(-\frac{n\,l\,f\,E}{L}\right)\right. \qquad 8.29$$

In the expression E/L refers to the field in the perpendicular direction of the surface where the oxide film grows and l is the distance between the equilibrium position of the cation and its position in the activated state (see Fig. 1.1b). k^{o}_{fg} is the film growth rate under zero field condition.

Now the field is assumed to be uniformly spread throughout the oxide electrolyte interface. The cation has to migrate from the *metal lattice to the first oxide layer* and then from *one oxide layer*

to the next oxide layer. Either of these steps can be the rate determining slow step. Cabrera and Mott [13] in fact proposed that the former step, that is, the migration at the metal oxide interface is the slow step. Verwey [14] proposed that the migration *in the film is the rate-controlling step.*

Equation 8.29 itself has two limiting conditions. If the field is very low $nf\,l\,E \ll L$, one can linearize the equation

$$\frac{dL}{dt} = k^{o}_{fg} \cdot \frac{nf\,l\,E}{L} \qquad 8.30$$

The expression on integration gives a relation in which L is linearly ted to $t^{1/2}$

$$L = At^{1/2} \qquad 8.31$$

This low field growth law is similar to the growth law that would be observed under solid state diffusion control.

Under high field conditions, the second exponential term in equation 8.29 may be neglected and one obtains

$$\frac{dL}{dt} = k^{o}_{fg}\, e^{nlfE/L} \qquad 8.32$$

This expression on integration at constant applied potential conditions yield a linear relation between $1/L$ and $-\log t$

$$\frac{1}{L} = A - B \log t \qquad 8.33$$

This is the popularly known inverse logarithmic law of oxide growth.

The current is related to the rate of growth by an equation that is identical to 8.26.

$$i = q_m \frac{dL}{dt} \qquad 8.26$$

However, the q_m is the charge required to oxidize one monolayer of metal atoms in the interfacial control model (Cabrera, Mott, Ref. 13). In the bulk migration control model (Vervey, Ref. 14) q_m would correspond to the charge required for the migration of one metal oxide layer. Such subtle features are used to distinguish the two models of oxide growth.

In general, oxide formation on valve metals such as tantalum, niobium and aluminium follow this high field conduction mechan-

ism. Oxide growth mechanism on metals such as Pt and Fe are still being critically evaluated. Exhaustive reviews on this subject are available [15–19]. However, most of them relate to work under potentiostatic conditions and evaluation of direct or inverse logarithmic growth law. As seen later, for LSV and CV studies, even the theoretical expressions are not comprehensively developed.

8.3 THE METHODS

As mentioned above, the formation and growth of bulk phases is an involved process and a number of phenomenological components are involved in each process model. Hence the theoretical analysis and even numerical simulation of results are much more difficult for these processes. Most of the methods employ constant potential conditions. The experimentally observed potentiostatic transients are then analyzed using these theories. However, many of these processes can be experimentally analyzed using LSV and CV techniques. At present these results are used to evaluate some qualitative features of the processes involved as shown later (Section 8.4). There is a hard-pressed need for developing the theoretical methodologies for such processes. In this section, the handful of attempts in these directions are briefly reviewed.

8.3.1 NUCLEATION-GROWTH-DIFFUSION MODEL

The model is composed of charge transfer, nucleation and growth of individual crystals. At longer times, one must consider the mass transfer effects [20]. Most of the simulation works correspond to potential step techniques.

A few attempts to extend the studies to linear sweep voltammetric techniques were also made. The voltammetric peaks are obtained in the forward sweep. The peak current characteristics are very similar to the diffusion controlled process. The i_p for example is proportional to $v^{1/2}$ or $v^{0.6}$ [21]. It has been concluded that from such criteria it may be difficult to differentiate this model from purely diffusion controlled models [22].

However, two characteristics are available to at least qualitatively differentiate this model from others. In the forward sweep, one should exert higher overvoltages for the formation of critical nuclei. But once such nuclei are formed, the growth process can continue

even at lower potentials. Hence in general, the current-voltage curve at the reverse sweep would cut across the current-voltage curve in the forward sweep. This type of curve-crossing or current-potential hysterisis has been considered as a positive evidence of nucleative processes for a very long time now (Section 8.4.1).

If the voltage is reversed in cyclic voltammetry, before the peak potential is approached in the forward sweep, one would in fact notice a current peak of the growth process in the reverse sweep as well. This type of behaviour is presented in Fig. 8.4. It has been quantitatively established that such a behaviour would be noticed both in the absence and in the presence of mass transfer effects [22].

More detailed investigations in this regard would be interesting.

8.3.2 CHEMICAL REACTION (POLYMERIZATION) MODEL

In the formation of conducting polymers, the charge transfer is followed by a polymerization reaction. The reaction scheme may be represented as the combination of equations 8.4 and 8.20. This scheme is similar to EC_{irr} mechanism presented in Chapter 5. In fact, these equations of EC_{irr} mechanism are widely used to investigate the conducting polymer formation mechanisms [23, 24].

However, one should note that the conducting polymer formation processes are different in at least two ways when compared with EC_{irr} processes considered in Chapter 5. In the polymerization reaction, the reaction order of the reactants (radical ions) are much higher when compared with polymerization reaction. This aspect should have a strong influence on the voltammetric behaviour, but it has not yet been investigated.

Secondly, the polymerization reaction takes place on the electrode surface. Hence the surface sites concentration would change as the polymerization reaction proceeds. In a two-dimensional surface process that was dealt with in Chapter 7, the available surface area would always decrease as the surface phase formation reaction proceeds. However, in the three-dimensional phase formation processes, the surface sites for polymerization may either decrease or increase. In conducting polymer formation, one would essentially expect a surface area increase and increase in the polymerization rate with time. This effect has indeed been noticed in potentiostatic transients by a number of workers [25, 26]. However, this effect is

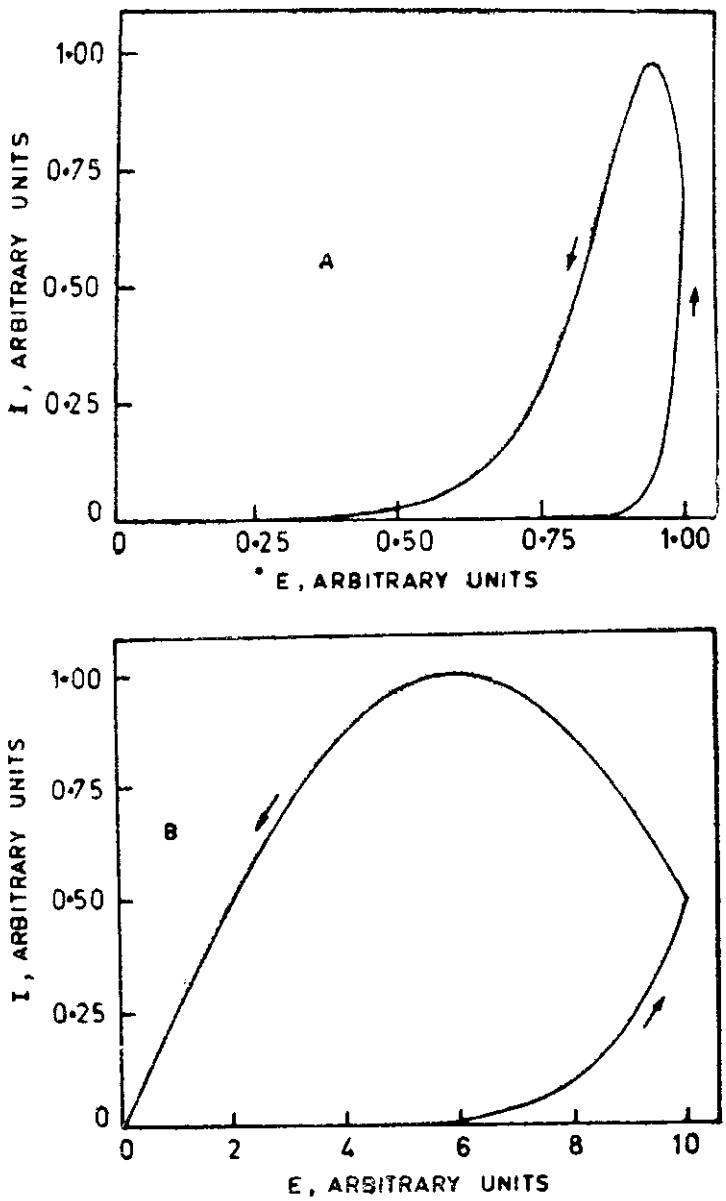

Fig. 8.4 Cyclic voltammetric response of nucleation-growth-diffusion model when the potential is reversed before the peak current; (a) irreversible (b) reversible growth rates. [From S Fetcher, CS Halliday, D Gater, M Westcott, T Lwin and G Nelson, J Electroanal Chem 159 (1983) 267].

not taken into consideration in the voltammetric experiments. Further investigations on this model are certainly called for.

8.3.3 INSULATING FILM FORMATION MODEL

If an insulating film is formed by an electrochemical reaction, the electron-transfer cannot take place on those areas where the film is

formed. As may be recalled the same type of assumptions were made in the investigations of monolayer formation processes by random adsorption model (Chapter 7). The same model can be effectively used for the study of insulating film formation processes.

However, two subtle aspects should be remembered. The charge q_m corresponding to monolayer coverage in the monolayer formation models (Chapter 7, Tables 7.1 to 7.3) would take a different meaning here. The q_m would correspond to maximum charge of the insulating film. The insulating film thickness may be much higher than the monolayer thickness. In fact, voltammetric results may be used to evaluate this parameter, knowing other variables presented in Table 7.1, for example.

Secondly, the monolayers formed would be dissolved in the reverse sweep. The insulating films, however, are formed by irreversible chemical reactions following charge transfer. Hence there would be no peak currents in the reverse sweeps of the cyclic voltammetric experiments. This in fact is the distinguishing criteria between the monolayer formation processes and insulating film formation processes.

8.3.4 DISSOLUTION-ADSORPTION MODEL

This discussion, so far, considered the surface processes without metal dissolution effects. A number of metallic corrosion and passive film formation processes are competitive processes where metal dissolution and solid phase growth processes take place simultaneously. Two different models are employed to interpret the passive film formation processes of this type. This section considers the dissolution-adsorption model and the next section (Section 8.3.5) deals with the dissolution-precipitation model.

In the dissolution-adsorption model, those commonly known as adsorption model, two competitive electron transfer processes take place simultaneously on the electrode surface.

$$M \rightleftharpoons M^{n+} + ne \qquad 8.1$$

$$M + X^{n-} \rightleftharpoons MX + ne \qquad 8.3$$

Reaction 8.1 would lead to metal dissolution process. Reaction 8.3 is a film formation process. Once film MX is formed on the surface, the metal dissolution cannot proceed on these sites.

The voltammetric responses for this model have been simulated in two brief investigations [27, 28]. The dissolution alone leads to the voltammetric response of Fig. 8.5.a. If the monolayer formation process alone takes place, the simulated response is similar to

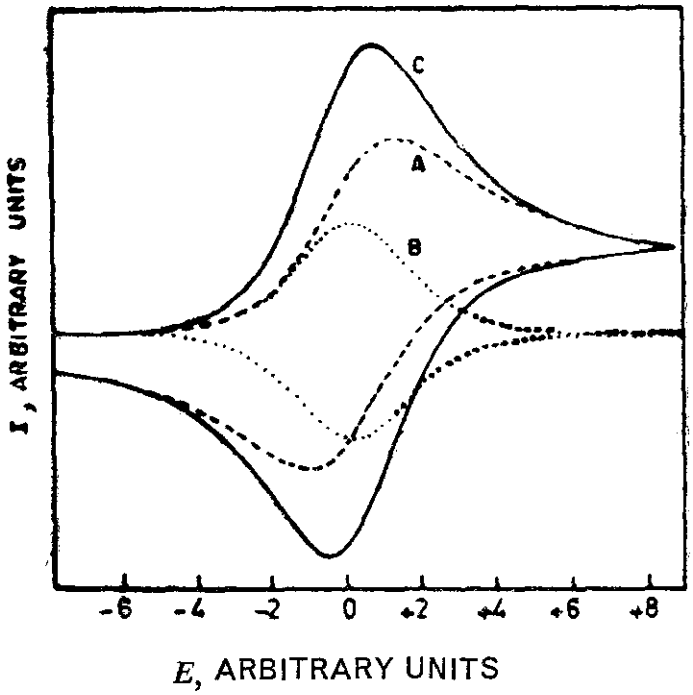

Fig. 8.5 Cyclic voltammetric response of dissolution-adsorption model under reversible charge transfer conditions. (a) Contribution by dissolution process, (b) contribution by adsorption process, (c) total current-potential response.
[From S Casadio, J Electroanal Chem 67 (1976) 123].

monolayer film formation process, represented in Fig. 8.5.b. The film formation effect influences the response due to metal dissolution which is presented in Fig. 8.5.a. The total current-potential response due to dissolution and adsorption processes is presented in Fig. 8.5.c. In these simulations, both the charge transfer processes were assumed to be reversible [27]. The effect of mass transfer, however, was taken care of. The voltammetric responses for slower charge transfer rates in the dissolution steps were also evaluated [28].

Apart from the fact that these works do not lead to any analytical expressions for the evaluation of rate and equilibrium parameters using i_p, E_p etc, the assumptions involved are very restrictive. First of all, the E^o values of reactions 8.27 and 8.28 can never be the same. Both are thermodynamically very different processes. Second-

ly, the effective electrode surface area is assumed to be constant throughout. However, as dissolution proceeds, the effective surface area certainly varies with time. Some method for incorporating these effects must be considered in further investigations.

Even with these restrictions, there is a notable feature in these studies [27, 28]. The overall response of the dissolution-adsorption model (Fig. 8.5.c.) is very similar to simple Nernstien diffusion-controlled processes considered in Chapters 3 and 4. Hence there is a possibility of misinterpretation among these two processes. One should investigate if very high sweep rate response would be purely or mostly due to adsorption process alone (Fig. 8.5.b). If this is so, as is most likely, this may be a distinguishing criterion between the two models.

The voltammetric response of solid state diffusion model also would be very similar to Fig. 8.5.c. However, in this case, the diffusion coefficients obtained from the voltammetric analysis would be very much smaller which would enable identification of this model.

8.3.5 DISSOLUTION-PRECIPITATION MODEL

The other passive film formation process model involves the dissolution step 8.1 coupled to a chemical precipitation reaction 8.18.

$$M \rightleftharpoons M^{n+} + ne \qquad 8.1$$

$$M^{n+} + X^{n-} \rightleftharpoons MX \qquad 8.18$$

The dissolution step is the same as discussed in the earlier section. But the precipitation reaction 8.18 is a chemical step. This step is potential independent.

In the original Muller's passivation model [29], the electron transfer was assumed to follow a linear current-potential relation, $E = IR$. This assumption is still held valid for such processes over a wide potential range. The inhibition is assumed to be due to the infinite resistance to charge transfer by the film MX.

Linear sweep voltammetric simulations of this model show the current-potential responses in the form of rectangular triangles as represented in Fig. 8.6 [30, 31]. The peak current and peak potentials are given by equations 8.34 and 8.35 respectively [30 - 32].

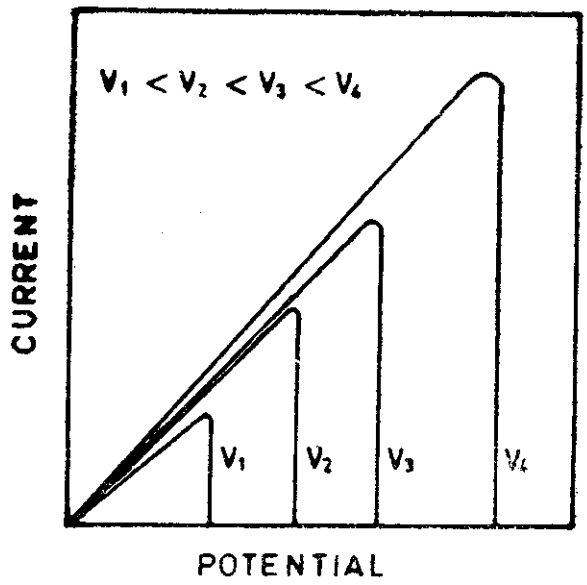

Fig. 8.6 Typical current potential response of dissolution-chemical precipitation model. Current as well as potential values are in arbitrary units.
[From AJ Calendra, NR Tacconi, R Pereiro and AG Arvia, Electrochim Acta 19 (1974) 901].

$$i_p = \left(\frac{nF\rho K}{M}\right)^{1/2} A\,(1-\theta_p)\,\nu^{1/2} \qquad 8.34$$

$$E_p = \left(\frac{nF\rho K}{M}\right)^{1/2}\left[\frac{\delta}{K} + R_0\,A\,(1-\theta_p)\right]\nu^{1/2} \qquad 8.35$$

In these equations, ρ, M and δ are the density, gram molecular weight and thickness of the passive film respectively and K and R_o are the conductivity of the solution in the pores and resistance of the solution outside the film respectively.

It is found that both the peak current and peak potentials are linearly related to the square root of sweep rate. These criteria as well as the very shape of the voltammogram would enable to distinguish this model from other ones.

Recently this model was extended to incorporate the growth through the film by assuming finite and lower resistivity values to the films [33]. The effect of growth over the film by further charge transfer reaction was also considered.

The very assumption of $E = IR$ type of relationship for charge transfer itself is questionable. It would be better to invoke a Butler-

Volmer relation or mass transfer relation to describe the charge transfer. The precipitation reaction may also be a slower one and the kinetics can influence mass transfer. These aspects require further consideration.

8.3.6 SOLID STATE PHASE GROWTH MODELS

Whatever be the mechanism of formation of the initial oxide film, after the formation of the first few layers, further oxide growth must follow some solid state growth mechanism. This should follow solid state diffusion, place exchange or migration mechanisms discussed.

The authors are not aware of any work that has attempted to develop and investigate the voltammetric responses for these models. One common feature of these models is the fact that the growth rate would decrease with increasing film thickness and increase with increasing anodic potential. When the potential is swept as in LSV, the growth rate and hence the current reaches an optimum limiting value, i_p. In recent studies, the following limiting current relationships with the sweep rate V are presented for different models [34].

i) Place exchange mechanism

$$i_l = K_1 . v \tag{8.36}$$

ii) Ionic migration-high field condition

$$i_l = K_2 + K_3 \log \left(-\frac{v}{i_l}\right) \tag{8.37}$$

iii) Ionic migration-low field-bulk control

$$i_l = K_3 . v^{1/2} \tag{8.38}$$

iv) Ionic migration-low field-interface control

$$i_l = K_u . \frac{v^{1/2}}{i_l^{1/2}} \tag{8.39}$$

In all these cases, the K_l values are constants that contain the model parameters. The methods of derivation of these results are not available from this work [34]. Perhaps these are obtained from the current expressions by substituting $E = vt$ and estimating the limiting value i_l as $t \to \alpha$. These expressions may be used for

qualitative characterization of mechanisms. However, more comprehensive simulation work and analytical expressions are certainly required.

8.4 THE PROCESS

Bulk formation and growth processes are investigated to a very great extent by a large number of research groups. Hence, even a brief and comprehensive review of all the factors involved would be a difficult task. In this section, only a brief review of recent works is mentioned to point out the directions of research in these areas. Some excellent reviews on each aspect, however, are quoted.

8.4.1 ELECTRODEPOSITION OF METALS

The importance of nucleation phenomena in the electrodeposition of metals on Hg and a number of other smooth substrates have been well established. Comprehensive reviews on nucleated metal deposition on Ag single crystals and other electrodes are available [10, 35]. At least three seminar proceedings deal exclusively with this electrocrystallization phenomenon [36 - 38].

Many of these works, however, employ potential step transients to characterize these processes. The rising portion of the current-time transient is taken as a clear indication of nucleative process. Quantitative analysis is also much more straightforward in these methods. Hence linear sweep and cyclic voltammetric methods are used only as qualitative tools to establish the presence of nucleative process. This may be seen by the hysterisis in the cyclic voltammogram. The cathodic current in the reverse sweep would be greater than the same in the forward sweep. Second indication is the presence of current maxima in the reverse sweep. Voltammograms of the type shown in Fig. 8.4 are observed in the electrodeposition of a number of metals on glassy carbon electrode [22].

Nucleation of metal crystallites seems to be an important first step when the metal deposit is formed on a foreign substrate. For example, the reduction potential for Cu on Pt is much more negative than the reduction potential of Cu on Cu electrode itself. An interesting voltammetric study in $AlBr_3$ containing aromatic hydrocarbon medium is presented in Fig. 8.7 [39, 40]. Such studies of electrodeposition of the same metal on different substrates

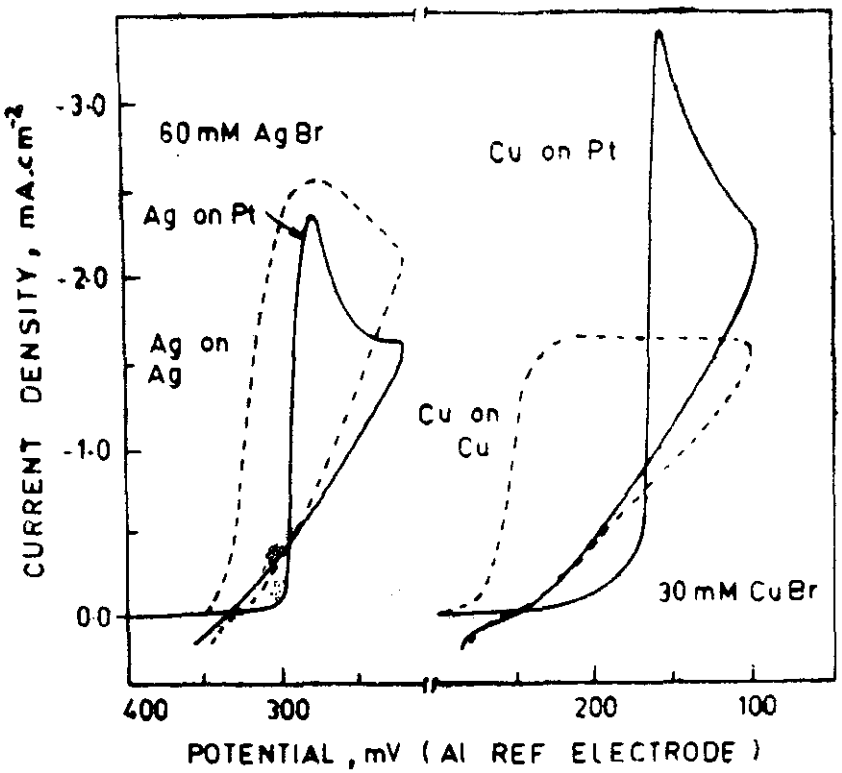

Fig. 8.7 Comparison of the initial potentials of deposition of Ag or Cu on Pt and on the respective metal. Sweep rate 12 mV/sec [From M Elam, E Peled and E Gileadi, J Electrochem Soc 131 (1984) 2058].

would certainly be another interesting way of nucleative electrodeposition processes.

8.4.2 FORMATION OF CONDUCTING/INSULATING POLYMER FILMS

For a very long period, the metals remained to be the best electrical conductors and organic polymers remained to be the best electrical insulators. With the advent of polyacetylene and related organic conducting polymers, a new thrust on preparation and characterization of these materials were noticed. In 1979, the polypyrrole with the conductivity in the range of 100 $(ohm\text{-}cm)^{-1}$ was prepared electrochemically [41, 42]. Extensive studies on substituted pyrroles [43] and characterization works [44] followed. In addition to aprotic solvents employed in the above works, aqueous solvents [26] and even low temperature melts [45] were employed in these studies.

The main cause for the high electrical conductivity of these materials is the conjugated double-bonded system in the polymeric

network. In addition to polypyrroles, a number of other related aromatic systems such as furans [46], thiophenes [47, 48], anilines [49, 50], aromatic diamines [51], indoles [52], polycyclic hydrocarbons [53], quinones [54] and even activated olefins [55] were found to give polymers of varying conductivity and mechanical stability. It is also possible to form conducting polymers of viologens [56], porphyrins [57] and silanes [58] by the same electropolymerization method. The reports in this field of research are really very extensive. A comprehensive review of recent developments is available [59]. A newly formed journal 'Synthetic Metals' contains a lot of reports in this field [60].

In most of these studies, LSV and CV methods are extensively used to evaluate formation potential, the thickness and the electrical conductivity of the films so produced. For example, in aqueous medium, the polypyrrole film formed at lower oxidation potential regions are good electrical conductors and allow film growth in the second as well as subsequent cycles (Figs. 4.8.a and b). However, if the formation potential is increased to more positive regions, the film produced becomes insulating and no film growth proceeds in the second cycle (Figs. 4.8.c and d). The peak current in the first sweep is used to evaluate the approximate number of electrons involved in the electro-oxidation process [24, 25]. In the case of polypyrrole, for example, n value greater than 2 is taken as an indication of the oxidized state of the film itself. However, as mentioned in Section 8.3.2, these studies neglect the increase in the surface area of the electrode during polymer film formations. Development and application of quantitative methods for the study of conducting polymers still remains to be a challenging problem in voltammetry.

One can also prepare and simultaneously characterize the electrical properties of purely insulating polymers by voltammetric methods. These insulating polymers are of interest in corrosion protection work. Detailed studies on phenol-based polymers may be quoted as examples [61–63]. The methods developed for monolayer formation are usually employed for the quantitative characterization of these types of films.

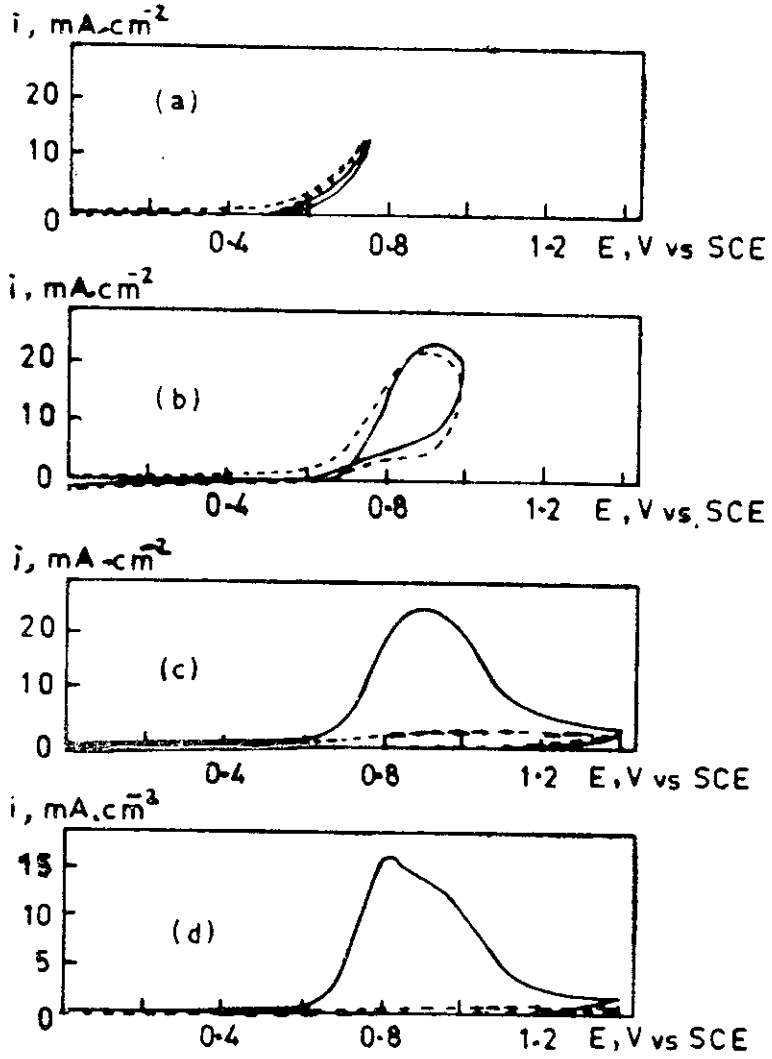

Fig. 8.8 The effect of the positive potential limit [curves (a) – (c)] and potential scan rate (d) on the CV of pyrrole (53 mM) in aqueous KNO_3 (1M). On Pt electrode. Scan rate 100 mV/sec (a) – (c) and 20 mV/sec (d) (——) First cycle; (.....) second cycle.

[From S Asavapiriyanont, GK Chandler, GA Gunawardena and D Pletcher, J Electroanal Chem 177 (1984) 229].

8.4.3 ANODIC FILM FORMATION AND GROWTH INVOLVING METAL DISSOLUTION

Compared with electrodeposition of metals and polymer films, the anodic film growth on metallic surfaces is much more involved. Even a clearcut classification of metals according to their film growth mechanisms is difficult. This section, therefore discusses the film

growth of all the metals where the metal-dissolution process is involved. The film growth on noble metals and valve metals is discussed in the next two sections.

Metals do undergo dissolution and film formation simultaneously. An excellent verification of this phenomenon is the oscillation noticed in the voltammetric curves. The current value shoots up whenever the pit is formed on a passive film and the current dips to a very low value whenever the pit is again closed by passivation. The oscillation behaviour on Sn electrode is presented in Fig. 8.9 [64]. Similar behaviour is also noticed on a few other metals such as zinc [65].

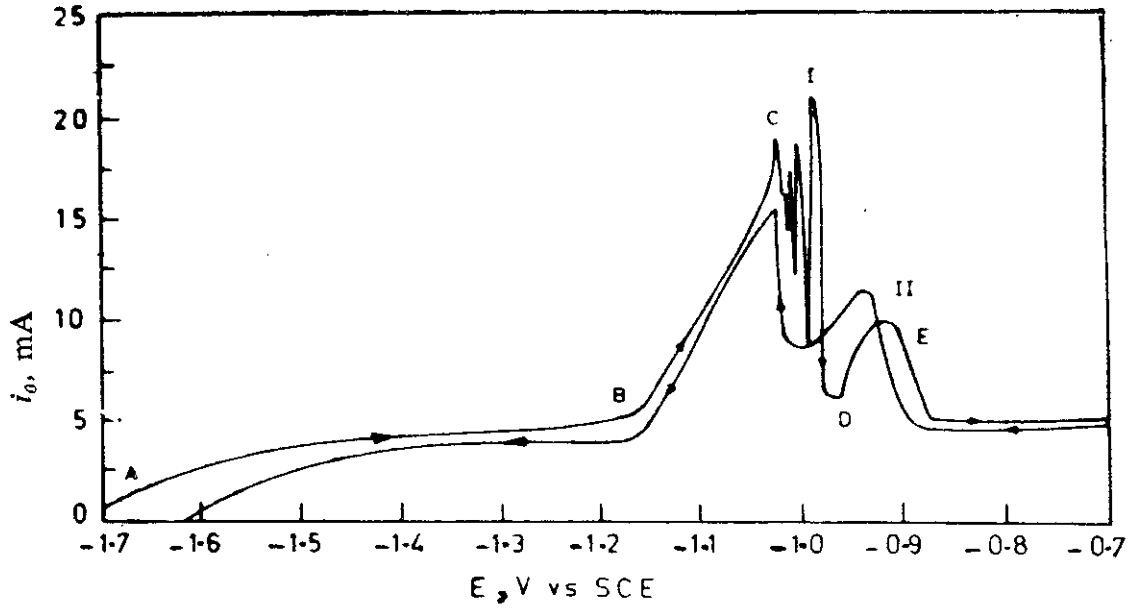

Fig. 8.9 CV of tin in 1.0 M NaOH solution. Sweep rate 1.21 mV/sec. [From VS Muralidharan, K Thangavelu and KS Rajagopalan, Electrochim Acta 28 (1983) 1611]

The oxide formation and growth on Fe electrode has been extensively investigated. LSV and CV studies cover a wide potential region embracing a host of processes such as Fe dissolution, OH^- ion adsorption, $Fe(OH)_2$ formation, further oxidation to FeOOH and solid state growth of the whole film. Naturally, the voltammograms contain a number of anodic as well as cathodic peak [34, 66–68]. Attempts have been made to evaluate the mechanism of oxide growth. However, much of the explanations remain qualitative, although distinguishing criteria between various growth mechanisms [34] have been employed. With the present day developments in electroche-

mical instrumentation, AC impedance methods are much more powerful in giving detailed information on a process like this which is composed of four or five different reactions with different time constants and potential dependencies [69, 70]. Even these studies are mainly concerned with the initial stages of passivation in acid media. More detailed investigations are certainly called for.

Apart from Fe, a number of other transition metal oxides have been investigated using LSV and CV. Voltammetric investigations on Co [71], Ni [72–74] and Bi [75] may be cited as examples. The general features of the voltammograms and the overall mechanistic pathways are quite similar. Fine details regarding the film structure, ionic solubility etc. are however different. Recently, the formation of FeOOH [76] and NiOOH films [77] on gold substrate from Fe^{2+} and Ni^{2+} species in solution were investigated. Since this is a single step process, more accurate and quantitative characterization of the films became possible. Such decoupling of process steps at the experimental level itself should be a very good basis for future work in this direction.

Even among noble metals, oxide formation on Ag and Cu seems to follow a dissolution-precipitation pathway. Detailed voltammetric investigations on the formation of oxide films on Ag [78–80] and Cu [81, 82] are available. Silver oxides of various stoichiometries are formed in the initial stages of oxidation [79]. Further oxide growth seems to proceed by solid state diffusion [80].

Many of the oxide couples discussed here such as $Zn/Zn(OH)_2$, $Fe(OH)_2/FeOOH$, $Ni(OH)_2/NiOOH$ and Ag/Ag_2O are important battery electrode couples. Another set of electrode reactions which are also important from battery angle are $Pb/PbSO_4$ and $PbSO_4/PbO_2$ couples involved in lead acid batteries. These electrode processes have been investigated using linear sweep and cyclic voltammetry [83–86]. The $Pb/PbSO_4$ reaction itself, for example, involves an interlayer of PbO formation in between lead and lead sulphate [83]. Recently, the effect of Sb addition in Pb on the overall electrode performance was investigated [87]. In general, in these battery electrodes, the electrical resistance in the pores ultimately restricts the formation, growth or electrochemical change of the solid phase. However, pore resistivity effects are noticed only after quite thick solid phase growth is noticed. In a few other cases such as graphite fluoride, the resistivity is noticed when the solid film is just one or

two monolayers thick [33]. The characteristics of battery electrodes can thus be evaluated from their voltammetric behaviour.

8.4.4 OXIDE GROWTH ON NOBLE METALS

In contrast with the oxide growth processes discussed above, Pt group metals and Au electrodes generally do not undergo dissolution to any appreciable extent. This is exactly the reason for the detailed investigations of monolayer oxide formation processes on these electrodes discussed in the last chapter (Section 7.4). At sufficiently anodic potentials and at sufficiently longer times, the oxide growth certainly continues beyond monolayer level. However, there is still no agreement regarding the mechanism of oxide growth in this region. For example, the oxide growth mechanism on Pt metal beyond 2.0 V is still under active discussion [88–92]. Inverse logarithmic as well as direct logarithmic laws are suggested to hold.

There are certain interesting features in the electrochemical oxide formation and growth on iridium electrodes. The oxide formed in the forward sweep is reduced back in the reverse sweep. But the iridium atoms do not take up their original places in the lattice points on the surface quickly. Hence, in a multisweep cyclic voltammetric experiment the oxide formation current shows a steady increase resulting in the formation of a very thick oxide film. Cyclic voltammetry seems to be the technique of choice for the study of this surface roughening mechanism of oxide growth. A large number of research reports are hence available on this specific topic [93–104]. When the thick oxide grows, the inner oxide layer becomes highly deficient in water content when compared with the oxide layer near the oxide-electrolyte interface. The redox behaviour of this outer and inner oxide layers or hydrous and anhydrous oxide layers are quite different. For example, one redox peak in a thin oxide layer splits into two redox peaks in the thick layers. These interesting phase changes are investigated at present using cyclic voltammetric and other techniques [103–104].

The formation of more than one type of oxide layer of the same oxidation state is certainly not specific to IrO_2 alone. In fact, such oxide phases were proposed and verified for Fe [105] and Ni [72] much earlier. Recently the existence of such oxides has been establi-

shed for Rh, Mo, W [106], Mn [107], Pt [108] and even Au [109]. These studies predominantly employ cyclic voltammetry.

8.4.5 OXIDE GROWTH ON VALVE METALS

Perhaps the valve metal oxide-electrolyte interface is the only one in electrochemistry that can hold a very high voltage drop beyond even 10.0V. The oxides formed on metals such as Nb, Ta and Hf are very stable dielectric materials. The voltage drop across such interfaces is indeed very high. The electrochemical oxidation on these

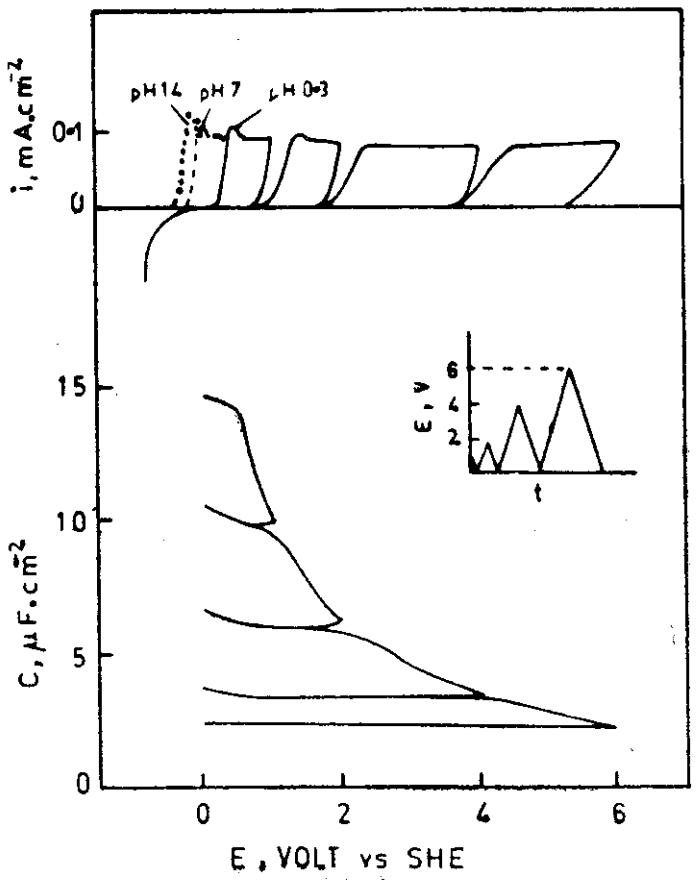

Fig. 8.10 CV curve of tantalum in 0.5M H_2SO_4 at 25°C. Sweep rate 25 mV/sec, upper curve; current density-voltage response, lower curve; capacity voltage response, inset; potential time programme, dashed line; borate buffer of pH 7.0, dotted line. NaOH medium of pH 14.

[From V Macagno and JW Schultze, J Electroanal Chem 180 (1984) 157]

metals follows high field conduction mechanism. The mechanistic studies mainly employ potentiostatic polarization experiments and have been extensively reviewed from time to time [15–19].

However, recently some voltammetric investigations on these types of interfaces have also appeared on the oxide growth of Ta [110, 111], Hf [112] and Al [113]. Typical cyclic voltammograms as well as simultaneous capacitance curves are presented in Fig. 8.10 [111]. One may notice that the oxide formation continues even beyond 6.0 V. Whenever the voltage is reversed at intermittent levels, the oxidation current immediately drops. On the reverse sweep, the oxides are not at all reduced. But cathodic hydrogen evolution starts on this surface.

In this chapter, only the formation and growth of three-dimensional films were treated. Their redox behaviour (Chapter 10) and electrocatalytic behaviour on other electrode reactions (Chapter 14) are treated later.

8.5 ANALYTICAL APPLICATIONS AND SCOPE

Studies on formation and growth of thin films are generally carried out with the primary objective of understanding the interfacial behaviour. Very few attempts to utilize the method for surface analysis have been made. The distinction between pure Fe and ferrophosphorus alloys can be clearly seen in their cyclic voltammetric responses, for example [114]. The voltammetric responses of tungsten bronzes may also be used as diagnostic criteria [115]. There is wide scope for evaluating surface composition of alloys by this method. Voltammetric methods may also be used to evaluate the electrodeposition characteristics and their dependence on substrate surface structure. An investigation of Cr deposition on Au can be cited as an example [116].

One would hope that more analytical applications of surface phase formation processes would be developed and used in the future.

REFERENCES

1 W Lorenz, Z Naturforsch 9a (1954) 716.

2 DA Vermilyea, J Chem Phys 25 (1956) 1254.

3 A Damjanovic and J O'M Bockris J Electrochem Soc 110 (1963) 1035.

4 J O'M Bockris and A Damjanovic, Modern Asp Electrochem 3 (1964) 224.

5 KJ Vetter, Electrochemical Kinetics, Academic Press, N York (1967).

6 M Fleischman, SK Rangarajan and HR Thirsk, Trans Farad Soc 63 (1967) 1240, 1251, 1256.

7 JA Harrison and HR Thirsk, Electroanal Chem 5 (1971) 67.

8 Ya B Zeldorich, J Exp Theoret Physics (USSR) 12 (1942) 525.

9 R Kaischew, Bull Acad Bulg Sci (Phys) 1 (1950) 100.

10 EB Budevski, Comp Treat in Electrochem 7 (1983) 399.

11 DA Vermilyea, Adv Electrochem and Electrochem Engg 3 (1963) 311.

12 N Sato and M Cohen, J Electrochem Soc 111 (1964) 512.

13 N Cabrera and NF Mott, Repts Prog Phys 12 (1949) 163.

14 FJW Verwey, Physica 2 (1935) 1059.

15 L Young, Anodic Oxide Films, Academic Press, N York (1960).

16 MJ Dignam, Oxides and Oxide Films, Vol. 1 (JW Diggle Ed) Marcel Dekker, N York (1973) 92.

17 AK Vijh, Electrochemistry of Metals and Semiconductors, Marcel Dekker, N York (1973).

18 A Damjonovic and AT Ward in Electrochemistry (J O'M Bockris, Ed), Butterworth, London (1976) 103.

19 MJ Dignam in Comprehensive Treatise Electrochem 4 (1981) 247.

20 S Fletcher, J Cryst Growth 62 (1983) 505.

21 S Fletcher, J Electroanal Chem 118 (1981) 419.

22 S Fletcher, CS Halliday, D Gates, M Westcott, T Lwin and G Nelson, J Electroanal Chem 159 (1983) 267.

23 RJ Waltman, AF Diaz and J Bargon, J Electrochem Soc 132 (1985) 631.

24 RJ Waltman, AF Diaz and J Bargon, J Phys Chem 88 (1984) 4343.

25 EM Genies, G Bidan and AF Diaz, 149 (1983) 101.

26 S Asvapriyanont, GK Chandler, GA Gunawardena and D Pleteher, J Electroanal Chem 177 (1984) 229, 245.

27 S Casadio, J Electroanal Chem 67 (1976) 123.

28 S Casadio, J Electroanal Chem 72 (1976) 243.

29 WJ Muller, Trans Faraday Soc 27 (1931) 737.

30 AJ Calandria, NR de Tacconi, R Pereiro and AP Arvia, Electrochim Acta 19 (1974) 901.

31 NR de Tacconi, AJ Calandia and AJ Arvia, Electrochim Acta 18 (1973) 571.

32 DD Macdonald, Transient Techniques in Electrochemistry, Plenum, N York (1977) Chapter 8.

33 D Devilliers, F Lantelme and M Chemla, Electrochim Acta 31 (1986) 1235.

34 A Wieckowski and E Ghali, Electrochim Acta 30 (1985) 1423.

35 M Fleischmann and HR Thirsk, Adv Electrochem and Electrochem Engg 3 (1963) 123.

36 Faraday Symp Chem Soc 12 (1976).

37 Electrocrystallization (R Weil and RG Barradas, Ed), Electrochem Soc Inc, New Jersey (1981).

38 Electrochim Acta 31 (1986).

39 M Elam, E Peled and E Gileadi, J Electrochem Soc 130 (1983) 585.

40 M Elam, E Peled and E Gileadi, J Electrochem Soc 131 (1984) 2058.

41 AF Diaz and KK Kanazawa, J Chem Soc Chem Commun (1979) 635.

42 KK Kanazawa, AF Diaz, RH Geiss, WD Gill, JF Kwak and JA Logan, J Chem Soc, Chem Commun (1979) 854.

43 AF Diaz, A Martinez and KK Kanazawa, J Electroanal Chem 130 (1981) 181.

44 EM Genies, G Bidan and AF Diaz, J Electroanal Chem 149 (1983) 101

45 PG Pickup and RA Osteryoung, J Amer Chem Soc 106 (1984) 2294.

46 S Pons and A Hinman, Electrochim Acta 29 (1984) 1251.

47 JH Kaufman, TC Chung, AJ Heager and F Whdl, J Electrochem Soc 131 (1984) 2092.

48 G Tourillon and F Garnier, J Electroanal Chem 161 (1984) 51.

49 AF Diaz and JA Logan, J Electroanal Chem 111 (1980) 111.

50 S Daolio, G Mengoli, M Musiani and P Bianco, Electrochim Acta 29 (1984) 1405.

51 RM Buchanan, GS Calabrese, TJ Sobieralski and MS Wrighton, J Electroanal Chem 153 (1983) 129.

52 RJ Waltman, AF Diaz and J Bargon, J Phys Chem 88 (1984) 4343.

53 RJ Waltman, AF Diaz and J Bargon, J Electrochem Soc 132 (1985) 631.

54 EW Daniel and W Robert, J Am Chem Soc 106 (1984) 355.

55 KW Willman and RW Munay, J Electroanal Chem 133 (1982) 211.

56 R Cieslinski aud NJ Armstrong, J Electroanal Chem 161 (1984) 59.

57 KA Macor and TG Spiro, J Amer Chem Soc 105 (1983) 5601.

58 AF Diaz and RD Miller, J Electrochem Soc 132 (1985) 834.

59 AF Diaz and J Bargon in Handbook of Conducting Polymers, Vol 1 (TA Skotheim, Ed), Marcel Dekker, N York (1986) 81.

60 Synthetic Metals, Elsevier, Amsterdam

61 F Bruno, MC Pham and JE Dubois, Electrochim Acta 22 (1975) 490.

62 MC Pham, PC Lacaze and JE Dubois, J Electroanal Chem 86 (1978) 147; 99 (1979) 331.

63 P Mourcel, MC Pham, PC Lacaze and JE Dubois, J Electroanal Chem 145 (1983) 467.

64 VS Muralidharan, K Thangavelu and KS Rajagopalan, Electrochim Acta 28 (1983) 1611.

65 JJ Podesta, RC Piatli and CV Arvia, J Electroanal Chem 154 (1983) 269

66 DD MacDonald and D Owen, J Electrochem Soc 120 (1973) 317.

67 A Wieckowski, E Ghali and H Ha Le, J Electrochem Soc 131 (1984) 2024.

68 VS Muralidharan and M Veerashanmugamani, J Appl Electrochem 15 (1985) 675.

69 M Keddam, OR Mattos and H Takenouti, J Electrochem Soc 128 (1981) 257.

70 M Keddam, OR Mattos and H Takenouti, Electrochim Acta 31 (1986) 1147.

71 TR Jayaraman, VK Venkatesan and HVK Udupa, Electrochim Acta 20 (1975) 209.

72 DM MacArthur, J Electrochem Soc 117 (1970) 729.

73 AE Bohe, JR Vilche and AJ Arvia, J Appl Electrochem 14 (1984) 645.

74 LD Burke and TAM Thomey, J Electroanal Chem 162 (1984) 101.

75 DE Williams and GA Wright, Electrochim Acta 21 (1976) 1009.

76 MM Lohrengel, K Schubert and JW Schultz, Werkstoffe und Korrosion 32 (1981) 13.

77 M Goledzinoski, S Haupt and JW Schultze, Electrochim Acta 29 (1984) 493.

78 J Ambrose and RG Barradas, Electrochim Acta 19 (1974) 781.

79 JMM Droog, PT Alderliesten and GA Brootsma, J Electroanal Chem 99 (1979) 173.

80 M Hepel and M Tomkiewicz, J Electrochem Soc 131 (1984) 1288.

81 De Gennero, MR Chalvo, SL Marchiano and AJ Arvia, J Appl Electrochem 14 (1984) 165.

82 L Brossard, Corrosion 40 (1984) 420.

83 D Pavlov, Electrochim Acta 13 (1968) 2051.

84 NA Hampson and JB Lakeran, J Electroanal Chem 107 (1980) 177; 108 (1980) 347; 112 (1980) 355.

85 S Fletcher and DB Mathews, J Appl Electrochem 11 (1981) 11, 23.

86 V Danel and V Plichen, Electrochim Acta 27 (1982) 771; 28 (1983) 781.

87 D Pavlov and B Monakhov, J Electroanal Chem 218 (1987) 135.

88 D James, J Electrochem Soc 116 (1969) 1681.

89 J Balej and O Spalek, Collect Czech Chem Commun 37 (1972) 499.
90 S Shibata, Electrochim Acta 17 (1972) 395.
91 VI Birss and A Damajanovic, J Electrochem Soc 130 (1983) 1688.
92 AA Yakovleva, IL Kubinova and Ya M Kolotyrkin, Elektrokhimiya 19 (1983) 723.
93 W Bold and M Breiter, Electrochim Acta 5 (1961) 169.
94 P Stonehast, H Angerstein-Kozlowska and BE Conway, Proc Roy Soc A 310 (1969) 541.
95 DAJ Rand and R Woods, J Electroanal Chem 55 (1974) 1, 13.
96 DN Buckley and LD Burke, JDS Faraday 1, 71 (1975) 1447.
97 S Gottesfeld and S Srinivasan, J Electroanal Chem 86 (1978) 89.
98 BE Conway and Mozota, Electrochim Acta 28 (1983) 1; 9.
99 MS Cruz, TF Otero and SU Zanartu, J Electroanal Chem 158 (1983) 375.
100 MF Yuen and I Lauks, Solid State Ion, 11 (1983) 19.
101 LD Burke and DP Whelan, J Electroanal Chem 162 (1984) 121.
102 LD Burke, JK Mulcahy and DP Whelan, J Electroanal Chem 163 (1984) 117.
103 V Birss, R Myers, H Angerstein-Kozlowska and BE Conway, J Electrochem Soc 131 (1984) 1502.
104 J Augustinski, M Koudelka, J Sanchez and BE Conway, J Electroanal Chem 160 (1984) 233.
105 M Nagayama and S Kawamura, Electrochim Acta 12 (1967) 1109.
106 LD Burke and EJM O'Sullivan, J Electroanal Chem 93 (1978) 11.
107 LD Burke and MJG Ahern, J Electroanal Chem 183 (1985) 183.
108 LD Burke and MBC Roche, J Electroanal Chem 159 (1983) 89.
109 LD Burke, MM McCarthy and MBC Roche, J Electroanal Chem 167 (1984) 291.
110 LL Odinets, E Ya Khanina and SS Chekmasova, Elektrokhimiya 19 (1983) 204.
111 V Macagno and JW Schultz, J Electroanal Chem 180 (1984) 157.
112 JW Schultz, Danzfuss, O Meyer and U Stimming, Materials Sci and Engg 69 (1985) 273.
113 E Palibroda, Electrochim Acta 28 (1983) 1185.
114 PJ Peerce-Landers and RJ Jasinski, J Electrochem Soc 130 (1983) 2380.
115 T Kishi, Y Muranushi and T Nagai, Surface Technol 21 (1984) 351.
116 JP Hoare, J Electroanal Chem 183 (1984) 87.